International Journal of Heat and Mass Transfer 52 (2009) 899–907

Contents lists available at ScienceDirect

International Journal of Heat and Mass Transfer

journal homepage: www.elsevier.com/locate/ijhmt

Three dimensional mixed convection in plane symmetric-sudden expansion: Symmetric flow regime

M. Thiruvengadam, B.F. Armaly *, J.A. Drallmeier

Department of Mechanical and Aerospace Engineering, Missouri University of Science and Technology, Rolla, MO 65409, USA

ARTICLE INFO

Article history:
Received 29 September 2007
Received in revised form 14 June 2008
Available online 29 August 2008

Keywords:
Laminar mixed convection
Internal flow
Separated flow
Heat transfer
3-D Numerical simulation

ABSTRACT

Three-dimensional simulations of laminar buoyancy assisting mixed convection in a vertical duct with a plane symmetric sudden expansion are presented to illustrate the effects of the buoyancy assisting force and the duct's aspect ratio on the flow and heat transfer. This geometry and flow conditions appear in many engineering applications, but 3-D heat transfer results have not appeared in the literature. This study focuses on the regime where the flow and thermal fields are symmetric in this geometry. The buoyancy force is varied by changing the heat flux on the stepped walls that are downstream from the sudden expansion, and the duct's aspect ratio is varied by changing the width of the duct while keeping the expansion ratio constant. Results are presented for duct's aspect ratio of 4, 8, 12, 16, and ∞ (2-D flow), and for wall heat fluxes between 5–35 W/m^2. The Reynolds number and the range of wall heat flux are selected to insure that the flow remains laminar and symmetric in this geometry and reverse flow does not develop at the exit section of the duct. Results for the velocity, temperature, and the Nusselt number distributions are presented, and the effects of the buoyancy force and the duct's aspect ratio on these results are discussed.

1. Introduction

The separation of flow and its subsequent reattachment due to sudden changes in geometry is a common phenomenon that occurs in many engineering applications such as in electronic cooling equipment, cooling of turbine blades, combustion chambers, and many other heat exchanging devices. Studies for isothermal laminar flow [1–6] in plane symmetric sudden expansion have shown that the flow is steady and symmetric for Reynolds number lower than a critical value, and asymmetric and steady for Reynolds number higher than the critical value. These studies also show that the critical Reynolds number increases with decreasing the aspect ratio and also with decreasing the expansion ratio of the duct. Tsui and Shu [7] and Alimi et al. [8] reported results for 2-D laminar mixed convection for the asymmetric flow regime. Thiruvengadam et al. [9] simulated the bifurcated 3-D forced convection, and in [10] they reported the effect of the buoyancy force and duct's aspect ratio on that asymmetric flow regime. The introduction of low levels of heating at the stepped walls (buoyancy assisting) caused the level of asymmetry in the flow to decrease for a fixed Reynolds number. The asymmetry ceases to exist in the flow and thermal fields, and a symmetric mixed convection flow regime develops at and beyond a critical level of buoyancy assisting force. The critical value of the buoyancy assisting force (or the wall heat flux) increases as the duct's aspect ratio increases thus reaching its maximum value for a duct with infinite aspect ratio (i.e. 2-D flow) for a fixed Reynolds number. For example, for the geometry and flow conditions that are considered in this study, i.e. duct's expansion ratio of two and Reynolds number of 800, symmetric buoyancy assisting mixed convection flow regime develops for wall heat flux larger than 6.21 W/m^2 for any of the aspect ratios. To the authors knowledge the effects of buoyancy force and duct's aspect ratio on the 3-D laminar symmetric mixed convection flow regime that develops in this geometry has not appeared in the literature and that motivated the present study.

2. Problem and solution procedure

This work, which focuses on the symmetric flow regime, is an extension of the work by Thiruvengadam et al. [9,10] where the asymmetric flow regime was examined. A schematic of the vertical plane symmetric sudden expansion geometry and the computational domain that is used in this simulation is presented in Fig. 1. The upstream duct height (h) is 0.02 m and the downstream duct height (H) is 0.04 m, respectively, resulting in expansion ratio (ER = H/h) of 2. The step height (S) is maintained at 0.01 m and the duct's width (W) is varied to examine the effect of upstream aspect ratio (AR = W/h) on the results. The origin of the coordinate system is located at the bottom corner of the sudden expansion as shown

* Corresponding author. Tel.: + 1 573 341 4601; fax: + 1 573 341 4609.
E-mail address: armaly@mst.edu (B.F. Armaly).

0017-9310/$ - see front matter © 2008 Elsevier Ltd. All rights reserved.
doi:10.1016/j.ijheatmasstransfer.2008.06.028

Nomenclature

AR	Upstream aspect ratio = W/h
ER	Expansion ratio = H/h
H	Duct height downstream from the sudden expansion
h	Duct height upstream from the sudden expansion
k	Thermal conductivity
L	Half width of the duct = $W/2$
Nu	Local Nusselt number = $q_w S/k(T_w - T_0)$
$Nu_{step,avg}$	Average Nusselt number on the stepped wall = $q_w S/k(T_{step,avg} - T_b)$
q_w	Wall heat flux = $-k\partial T/\partial n$ at the wall
Re	Reynolds number = $2\rho u_0 h/\mu$
S	Step height
T	Temperature
T_b	Bulk fluid temperature = $\frac{\int_0^W \int_0^H u(x,y,z)T(x,y,z)\mathrm{d}y\mathrm{d}z}{\int_0^W \int_0^H u(x,y,z)\mathrm{d}y\mathrm{d}z}$
T_w	Local wall Temperature
T_0	Inlet fluid temperature
$T_{step,avg}$	Average stepped wall temperature = $\frac{1}{L}\int_0^L T_{w,step}\mathrm{d}z$
$T_{side,avg}$	Average side wall temperature = $\frac{1}{H}\int_0^H T_{w,\,side}\mathrm{d}y$
u	Velocity component in the x-coordinate direction
u_0	Average inlet velocity
v	Velocity component in the y-coordinate direction
W	Width of the duct
w	Velocity component in the z-coordinate direction
x	Streamwise coordinate
x_u	Locations where the streamwise velocity gradient is zero ($\partial u/\partial y_{at\ wall} = 0$)
y	Transverse coordinate
z	Spanwise coordinate

Greek symbols

β	Volumetric coefficient of thermal expansion
μ	Dynamic viscosity
ρ	Density

in Fig. 1. The directions of the streamwise (x), transverse (y), and spanwise (z) coordinates are shown in that figure. The length of the computational domain is 1.0 m downstream and 0.02 m upstream of the sudden expansion, respectively, i.e. $-2 \leqslant x/S \leqslant 100$. This choice is made to insure that the flow at the inlet section of the duct ($x/S = -2$) is not affected by the sudden expansion in geometry, and reverse flow does not develop at the exit section of the duct (i.e. starved flow condition at the higher wall heat flux) and can be treated as fully developed. The governing equations for steady laminar, incompressible, three-dimensional, buoyancy assisting mixed convection with constant properties are formulated for the continuity, momentum, and energy conservation. Thermal buoyancy effects are modeled using the Boussinesq approximation. Details of the governing equations can be found in Li and Armaly [11] who studied laminar mixed convection

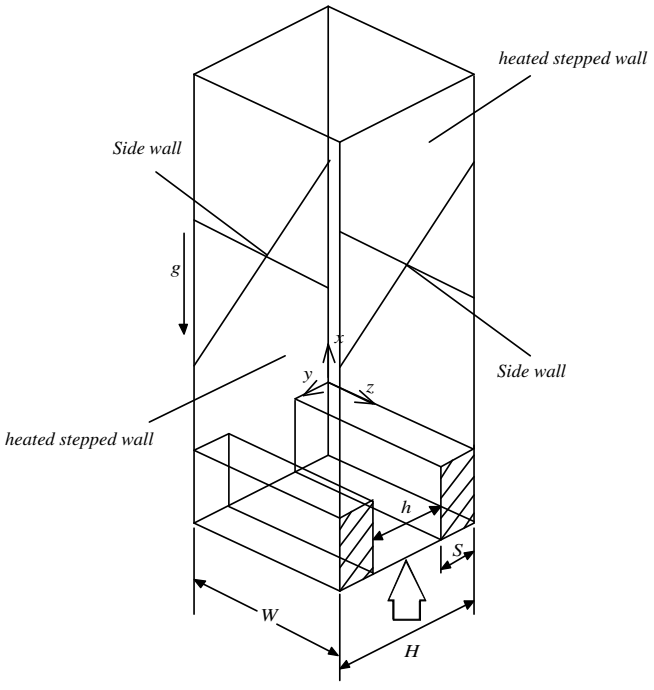

Fig. 1. Schematic of the computational domain.

effects in 3-D backward facing step and these equations will not be re-stated here due to space limitations. The full elliptic 3-D coupled governing equations are solved numerically using finite volume method to simulate the flow and the temperature fields in this computational domain.

The physical properties are treated as constants and evaluated for air at the inlet temperature of $T_0 = 20\ ^\circ C$ (i.e. density (ρ) is 1.205 kg/m^3, specific heat (C_p) is 1005 J/kg K, dynamic viscosity (μ) is 1.81×10^{-5} kg/m s, thermal conductivity (k) is 0.0259 W/m K, and volumetric coefficient of thermal expansion (β) is 0.00341 l/K). Inlet flow (at $x/S = -2$, $1 \leqslant y/S \leqslant 3$, for all z) is considered to be isothermal ($T_0 = 20\ ^\circ C$), steady, and fully developed. The distribution for the isothermal fully developed streamwise velocity component (u) in rectangular duct that was used in this study is given by Shah and Bhatti [12] and is not repeated here due to space limitations. The other velocity components (transverse (v) and spanwise (w)) are set to be equal to zero at that inlet section. The no-slip boundary condition (zero velocities) is applied to all of the wall surfaces. Uniform and constant wall heat flux (q_w) is specified at the two stepped walls (at $y/S = 0$ and 4, $0 \leqslant x/S \leqslant 100$, for all z), while other walls (side walls) are treated as adiabatic surfaces. The magnitude of that wall heat flux is varied between 5–35 W/m^2 while keeping the Reynolds number ($Re = 2\rho u_0 h/\mu$, where u_0 is the average inlet velocity) fixed at 800 in order to investigate the effects of the buoyancy assisting force on the flow and heat transfer. Similarly, the magnitude of the wall heat flux is fixed at 15 W/m^2, and the Reynolds number is fixed at 800 while the aspect ratio is varied in order to investigate its effect on the flow and heat transfer. Due to the symmetry of the flow and thermal fields in the spanwise direction for the stated conditions in this geometry, the width of the computational domain is chosen as half of the actual width of the duct, $L = W/2$, and symmetry boundary conditions are applied at the center width of the duct, i.e. at $z = L$, $w = 0$, and the gradient of all the other quantities with respect to z are set equal to zero. Fully developed flow and thermal conditions are imposed at the exit section (at $x/S = 100$, for all y and z) of the calculation domain.

Numerical solution of the governing equations and boundary conditions are performed by utilizing the commercial computational fluid dynamics (CFD) code FLUENT 6.2. The mesh is generated using FLUENT's preprocessor GAMBIT. Hexahedron volume elements are used in the simulation. The residual sum for each of the conserved variables is computed and stored at the end of each iteration, thus recording the convergence history. The convergence

criterion required that the scaled residuals be smaller than 10^{-10} for the mass and the momentum equations and smaller than 10^{-11} for the energy equation. Calculations are performed on DELL workstation, and the CPU time for converged solution for $Re = 800$ is approximately 24 h. The SIMPLEC algorithm is used for the pressure velocity coupling, and the momentum and energy equations are discretized with the Second Order Upwind scheme in order to improve the accuracy of the simulations. Detailed descriptions of the CFD code may be found in the FLUENT manual.

The computational grid distribution is selected to insure high density near the bounding walls and in the regions of the sudden expansion where high gradients exist, in order to insure the accuracy of the simulation. Grid independence tests were performed using different grid densities for $Re = 800$ for all aspect ratios and the results of the study are reported in [10]. From the grid study for AR = 8 a grid of $(220 \times 64 \times 50)$ is used downstream of the sudden expansion ($0 \leqslant x/S \leqslant 100$) and a grid of $(20 \times 32 \times 50)$ is used upstream of the sudden expansion ($-2 \leqslant x/S \leqslant 0$) for half of the duct's width ($0 \leqslant z/L \leqslant 1$). This grid size is used for aspect ratios smaller or equal to 8 ($AR \leqslant 8$). A grid of $(20 \times 32 \times 60)$ upstream of the sudden expansion and a grid of $(220 \times 64 \times 60)$ downstream of the sudden expansion provides grid independent results for aspect ratio AR = 16 and this grid size is used for 8 < AR $\leqslant$ 16. The results for code validation could be found in Thiruvengadam et al. [9,10].

3. Results and discussion

3.1. Effects of buoyancy

The effects of buoyancy are examined by fixing the aspect ratio to four (AR = 4), expansion ratio to two (ER = 2), and the Reynolds number to 800 ($Re = 800$) while changing the magnitude of the constant and uniform wall heat flux (q_w) from 5 to 35 W/m^2. Results for other aspect ratios and Reynolds numbers exhibited similar trend and for that reason they are not presented in this study. Thiruvengadam et al. [10] have shown that for this specific geometry (ER = 2, AR = 4, and $Re = 800$) a symmetric flow develops when the wall heat flux is larger than 3.52 W/m^2 and asymmetric flow develops for smaller wall heat flux. The complex flow behavior that develops downstream of the sudden expansion has been discussed in detail by Thiruvengadam et al. [9,10]. A "jet-like" flow develops adjacent to the side walls, in the separating shear layer after the sudden expansion in this geometry, which impinges on the stepped walls to form several recirculation flow regions.

The general flow features in this geometry are presented in Fig. 2 by streamlines at different spanwise planes near the side walls. The primary recirculation flow region that develops downstream from the sudden expansion can be clearly seen in this figure, and its size decreases as the distance from the sidewall toward the center width of the duct increases. The effect of the wall heat flux on the size of the recirculation flow region is presented in Fig. 3 by a presentation of the x_u-lines. The x_u-lines represent the locations where the streamwise component of the wall shear stress is zero ($\mu \frac{\partial u}{\partial y}_{wall} = 0$), and that definition is commonly used to identify the reattachment length in two-dimensional separated flow. The locations of the "jet-like" flow impingement on the stepped wall are shown in Fig. 3 for different levels of wall heat flux. When the heat flux is increased to 35 W/m^2 there is no "jet-like" flow impingement on the stepped walls. Increasing the wall heat flux decreases the size of the recirculation flow region. This is due to the buoyancy induced streamwise velocity component in the recirculation flow region which increases with increasing buoyancy force. The results in Fig. 3 show that for low wall heat flux of 5 and 10 W/m^2, two reattachment lines are identified with

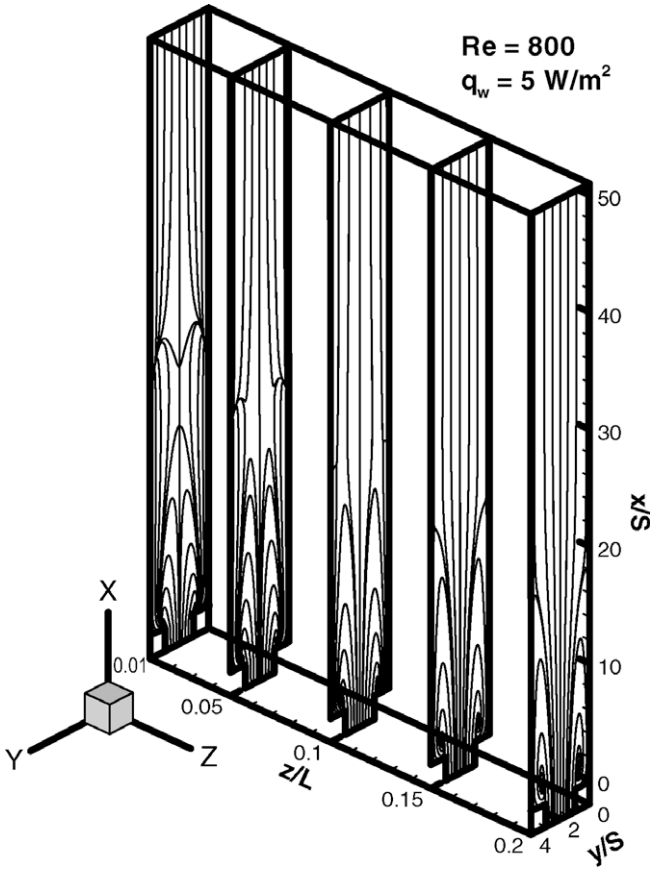

Fig. 2. General flow behavior for $q_w = 5$ W/m^2.

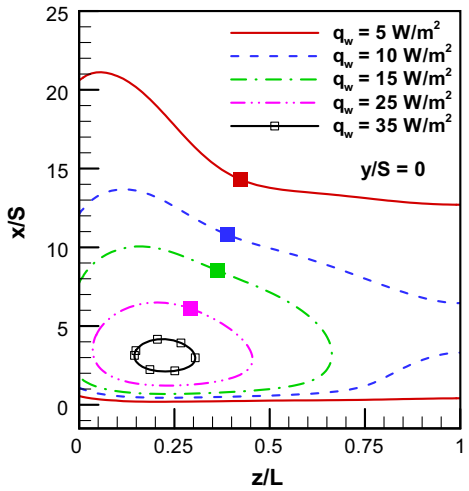

Fig. 3. Distribution of the x_u lines on the stepped wall (■ Location of the "jet-like" flow impingement).

one appearing very close to the sudden expansion region. Increasing the wall heat flux causes one of the reattachment line to move downstream and the other reattachment line to move upstream. Higher wall heat flux causes the recirculation flow region to start lifting partially up and away from the stepped wall at the center width of the duct. Further lifting of the recirculation flow region away from the stepped wall continues as the wall heat flux continues to increase.

The effect of wall heat flux on the transverse distributions of the streamwise velocity and temperature at the center width of the

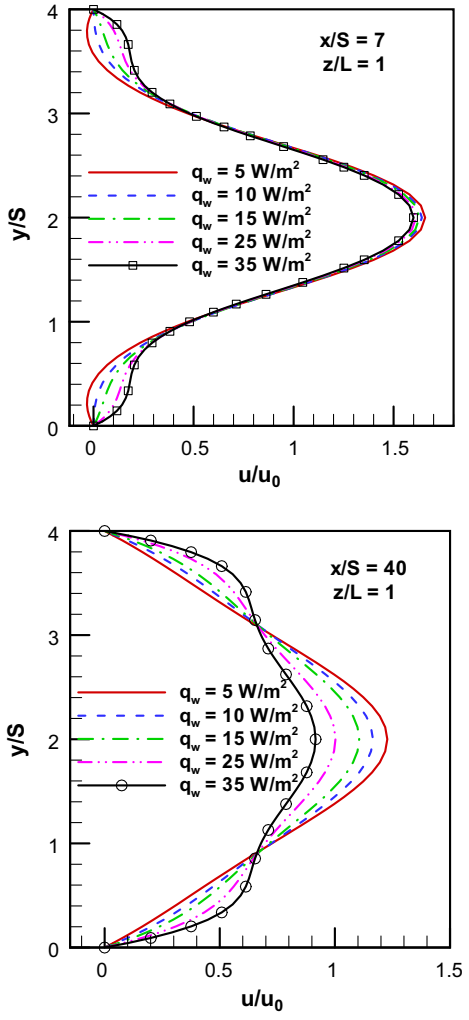

Fig. 4. Streamwise velocity distribution.

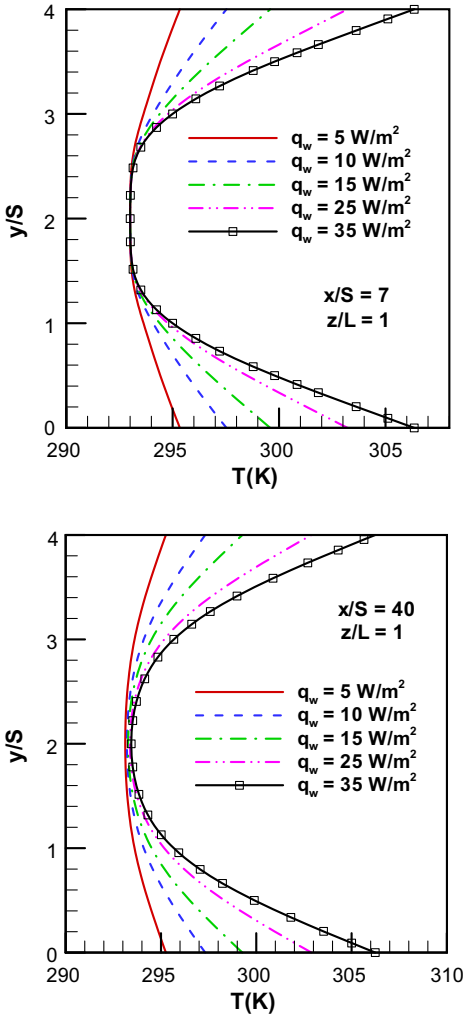

Fig. 5. Fluid temperature distribution.

duct and at streamwise locations inside ($x/S = 7.0$) and outside the recirculation flow region ($x/S = 40$) are presented in Figs. 4 and 5. The velocity distribution exhibits similar behavior but the effect of buoyancy is more pronounced at larger streamwise location. Increasing the buoyancy force increases the velocity and its gradient near the stepped walls, and in order to maintain mass balance its magnitude at the center height of the duct decreases. Higher buoyancy force results in higher wall and fluid temperature as shown in Fig. 5. The temperature at the center height of the duct, however, is not affected significantly by the increasing buoyancy force in the range of parameters that are examined in this study at the selected streamwise location.

The resulting spanwise distributions of the wall temperature are presented for a fixed wall heat flux ($q_w = 15$ W/m^2) at different streamwise locations, and for different wall heat flux at a fixed streamwise location ($x/S = 7$) in Fig. 6. Significant wall temperature variations develop in the spanwise direction, particularly at high wall heat flux. It is interesting to note the difference between the distributions at $x/S = 1$ and at $x/S = 40$. In the fully developed flow regime the wall temperature near the sidewall is higher than that at the center width of the duct, and that is due to the higher streamwise velocity at the center width of the duct. On the other hand near the sudden expansion at $x/S = 1$, the lower wall temperature is near the sidewall and that is due to the relatively strong recirculation flow that develops near the bottom corner and adjacent to the side wall in this geometry. The relatively lower velocity that develops at the center width of the duct at that plane ($x/S = 1$) results in a higher temperature at the center width of the duct. The local minimum that appears in the other distributions is due to the "jet-like" flow impingement on the stepped wall, and a higher wall heat flux results in a higher wall temperature.

The effect of wall heat flux on the streamwise distribution of local Nusselt number (based on the inlet fluid temperature) is presented at $z/L = 0.1$ and 1.0 in Fig. 7. The expected streamwise distribution of a developing peak in the neighborhood of the reattachment region followed by a gradual decrease with increasing distance from the sudden expansion is observed. The results show that a higher Nusselt number occurs near the side wall ($z/L = 0.1$) than at the center width of the duct. Higher wall heat flux is associated with a higher Nusselt number. The local minimum that develops near the sudden expansion in these distributions for higher wall heat flux is due to the partial lifting of the recirculation flow region away from the stepped wall as shown in Fig. 3 and the resulting higher fluid temperature that flows adjacent to the wall in that region. The difference in the local Nusselt number distributions at $z/L = 0.1$ and at $z/L = 1$ demonstrates the significant effect of the three-dimensional flow behavior on the results.

The effect of wall heat flux on the streamwise distributions of the average stepped wall temperature ($T_{\text{step,avg}}$) and the average side wall temperature ($T_{\text{side,avg}}$) are shown in Figs. 8 and 9, respec-

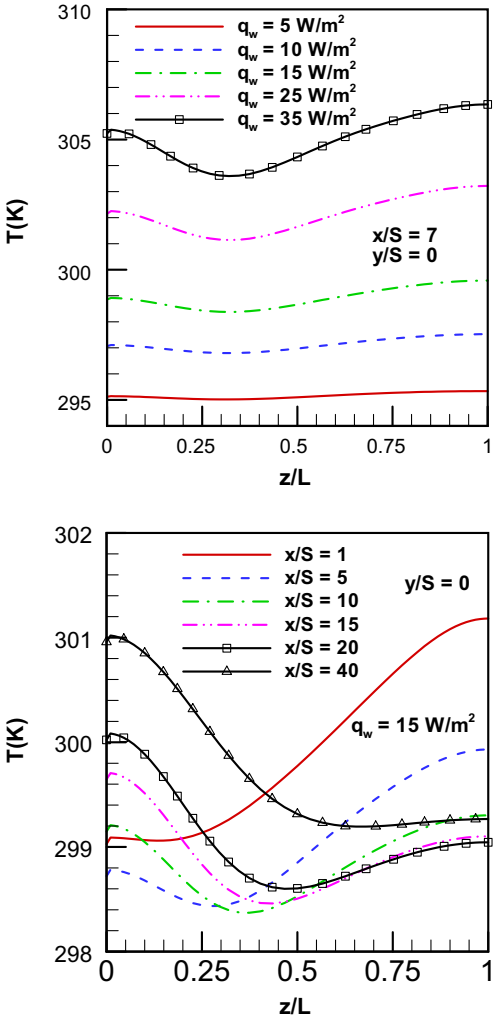

Fig. 6. Spanwise distribution of the stepped wall temperature.

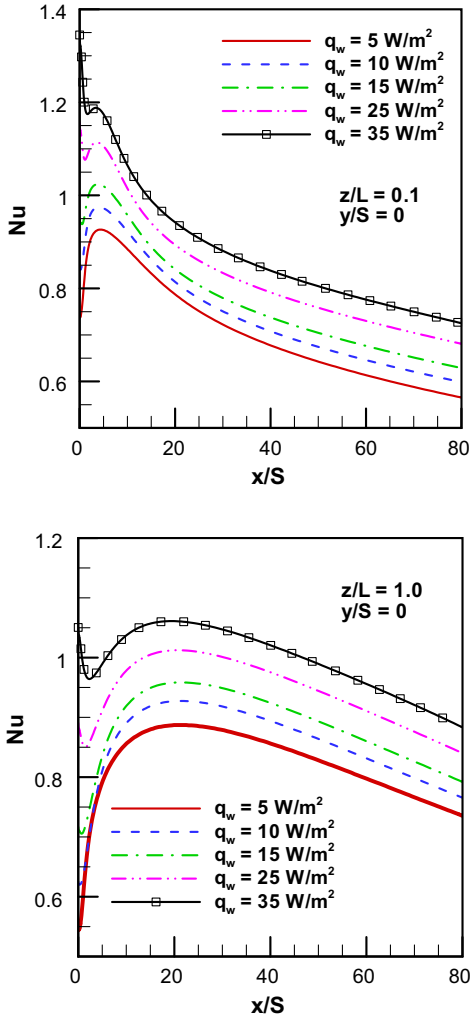

Fig. 7. Local Nusselt number distribution.

tively. These temperatures increase with increasing wall heat flux and show a linear increase downstream from the reattachment region that is similar to what is observed in fully developed flow region in a duct. The average sidewall temperature is lower than the average stepped wall temperature and the "jet-like" flow impingement is associated with the minimum that appears in these distributions. The effect of wall heat flux on the streamwise distribution of the bulk fluid temperature (T_b) is shown in Fig. 10. It increases with increasing wall heat flux and streamwise distance, and develops a constant slope after the reattachment region. The small non-linearity that appears in that distribution after the sudden expansion is due to the recirculation flow that develops in that region.

The effect of wall heat flux on the streamwise distribution of the average Nusselt number on the stepped wall (based on the bulk fluid temperature) is presented in Fig. 11. Its magnitude increases with increasing wall heat flux and it has a linear variation in the fully developed region of the flow. For the lower wall heat flux cases of $q_w \leqslant 15\ W/m^2$, its magnitude increases rapidly with distance from the sudden expansion then gradually continues to increase as the distance increases. The results in Fig. 11 show a different trend than those in Fig. 7 and that is due to the fact that the bulk fluid temperature, that varies with distance from the sudden expansion, is used in the calculations of the average Nusselt number (Fig. 11) while the inlet fluid temperature, that is fixed at 20 °C, is used in the calculations of the local Nusselt number (Fig. 7).

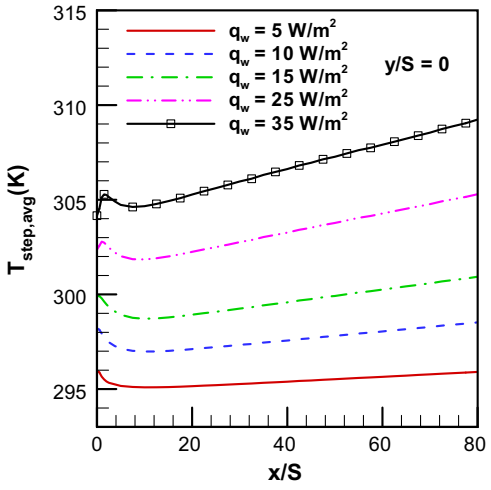

Fig. 8. Streamwise distribution of the average stepped wall temperature.

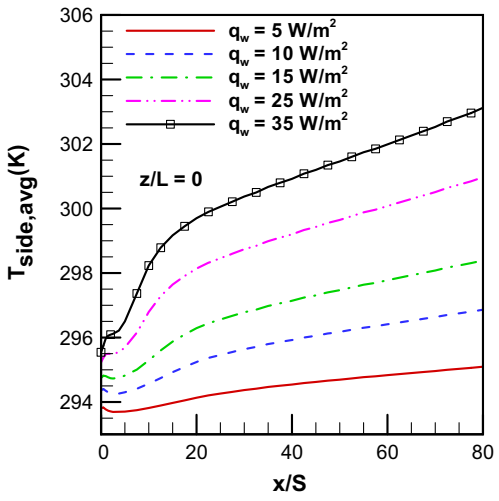

Fig. 9. Streamwise distribution of the average side wall temperature.

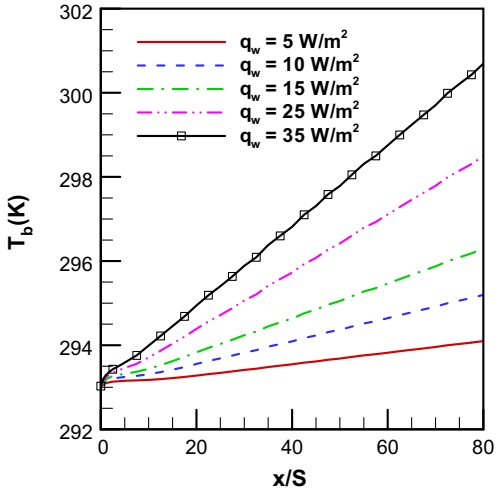

Fig. 10. Streamwise distribution of the bulk fluid temperature.

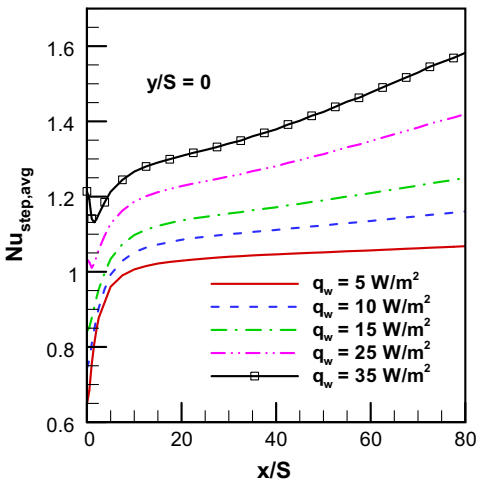

Fig. 11. Streamwise distribution of the average Nusselt number.

3.2. Effects of aspect ratio

The effect of aspect ratio on the flow and heat transfer in this geometry is examined by keeping the expansion ratio, the Reynolds number and the wall heat flux constant at ER = 2.0, Re = 800, and q_w = 15 W/m^2, respectively, while varying the aspect ratio (AR) between 4 and infinity (2-D) by selecting different duct's width of the duct. The effect of the aspect ratio on the size of the recirculation flow region is shown in Fig. 12 by presenting the distribution of the x_u-lines. These results show that the recirculation flow region is totally attached to the stepped wall for the cases with higher aspect ratios but start to partially lift away from the stepped wall as the aspect ratio decreases. These results show that a higher level of wall heat flux is required to partially lift the recirculation flow region away from the stepped wall as the aspect ratio increases. The "jet-like" flow impingement locations that are identified in this figure move downstream and closer to the side wall as the aspect ratio increases.

The effect of aspect ratio on the transverse distribution of the streamwise velocity component at the center width of the duct and at streamwise locations of x/S = 7 and 40 are presented in Fig. 13. A smaller reattachment length and a higher center line velocity develop for smaller aspect ratios. The effect of the aspect ratio on the fluid temperature at the center width of the duct at these planes is negligible, and for that reason it is not presented graphically. The effect of aspect ratio on the spanwise distribution of the wall temperature at x/S = 7 is presented in Fig. 14. The minimum that appears in these distributions close to the side wall is due to the "jet-like" flow impingement on the wall in that region. That minimum decreases and moves closer toward the center width of the duct as the aspect ratio decreases.

The streamwise distribution of the local Nusselt number (based on the inlet fluid temperature) at a location near the side wall (z/L = 0.1) and at the center width of the duct (z/L = 1) is presented in Fig. 15. A peak develops in its distribution near the reattachment region and that peak increases as the aspect ratio increases. The aspect ratio continues to significantly influence the results near the side wall for ducts with large aspect ratio. The 2-D simulation results are presented in these figures for comparison and they show that the results from the AR = 16, relatively wide duct, are approaching those from the 2-D simulations at the center width of the duct but that is not the case near the side wall. The relatively lower stepped wall temperature that develops near the side wall,

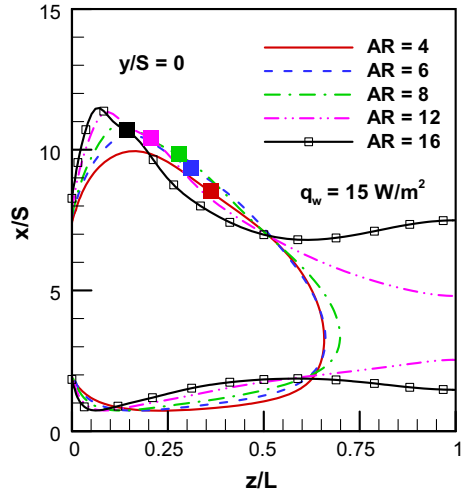

Fig. 12. Effect of aspect ratio on the distribution of the x_u lines (■ Location of the "jet-like" flow impingement).

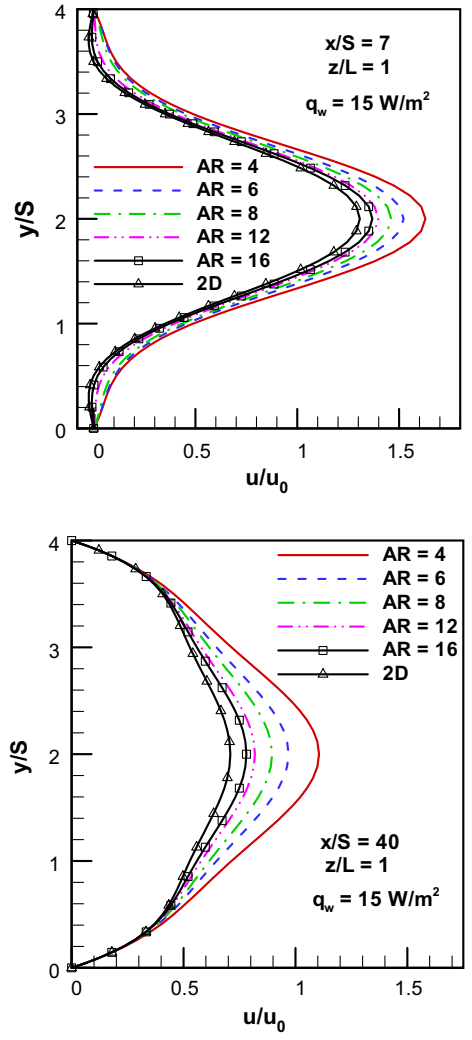

Fig. 13. Effect of aspect ratio on the transverse distribution of the streamwise velocity.

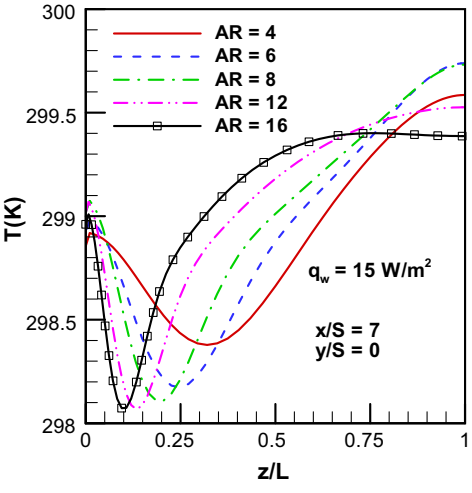

Fig. 14. Effect of aspect ratio on the spanwise distribution of the stepped wall temperature.

as compared to its center width value (3-D effects), contributes to this behavior and that effect continues to be significant in this region for ducts with large aspect ratio. In the fully developed flow

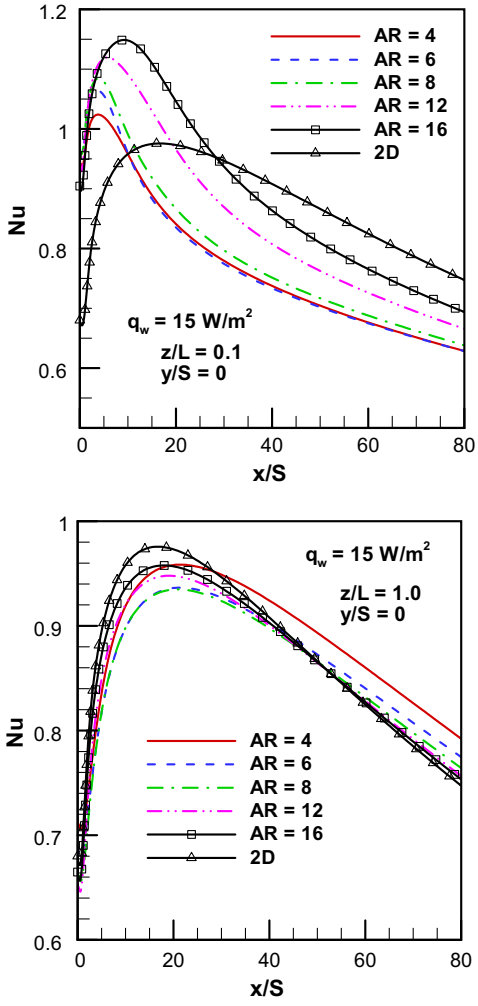

Fig. 15. Effect of aspect ratio on the local Nusselt number distribution.

region the local Nusselt number increases with the increase in the aspect ratio near the side wall, but that trend is reversed at the center width of the duct as shown in Fig. 15. The maximum local Nusselt number increases and its location moves closer toward the side wall as the aspect ratio increases as can be seen from the results that are tabulated below for wall heat flux of 15 W/m^2.

Magnitudes and locations of maximum local Nusselt number (for q_w = 15 W/m^2 & Re = 800)

x/S	y/S	z/L	Nu_{max}	AR
8.494	0	0.3464	1.079	4
8.752	0	0.2707	1.122	6
8.752	0	0.2053	1.14	8
9.560	0	0.1475	1.153	12
9.840	0	0.1069	1.154	16
16.362	0		0.976	2-D

The effect of the duct's aspect ratio on the streamwise distribution of the average stepped wall temperature ($T_{step,avg}$) is presented in Fig. 16. These results show that this temperature decreases rapidly after the sudden expansion, reaching a minimum near the flow reattachment region, and increasing linearly in the fully developed flow region. The results show that the average stepped wall temperature is not affected significantly by the duct aspect ratio. There is a slight decrease with increasing the aspect ratio in the fully

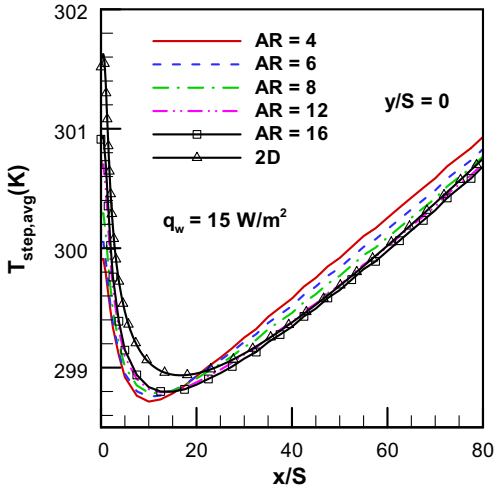

Fig. 16. Effect of aspect ratio on the streamwise distribution of the average stepped wall temperature.

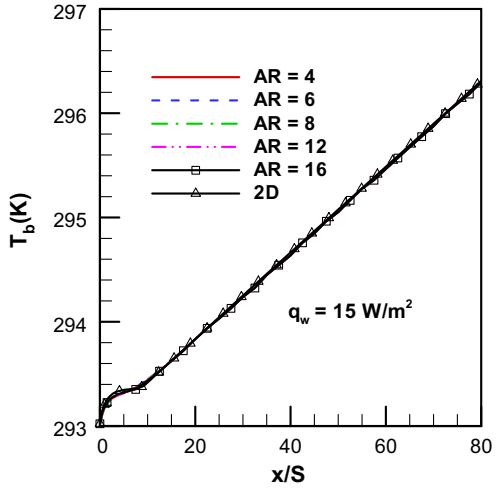

Fig. 17. Effect of aspect ratio on the streamwise distribution of the bulk fluid temperature.

developed flow region. The streamwise distribution of the bulk fluid temperature (T_b) is presented in Fig. 17 and it exhibits a linear behavior after the reattachment region, and as expected it is independent of the aspect ratio. The changes in the streamwise distribution of the average side wall temperature due to changes in the aspect ratio is insignificant for aspect ratio larger than 6 and for that reason that behavior is not presented graphically.

The effect of the aspect ratio on the streamwise distribution of the average Nusselt number ($Nu_{step,avg}$) is presented in Fig. 18. The results show a steep increase in its magnitude in the recirculation flow region followed by a lower rate of increase after that region. The local maximum that appears normally in the local Nusselt number distribution (that uses the constant inlet fluid temperature in its definition) as shown in Fig. 15, does not appear in the distribution of the average Nusselt number ($Nu_{step,avg}$) due to the use of the bulk fluid temperature in its definition. These results approach the 2-D values as the aspect ratio increases. A slightly higher average Nusselt number develops in the region near the sudden expansion for ducts with lower aspect ratio but that trend is reversed in the fully developed region of the flow. The change in the aspect

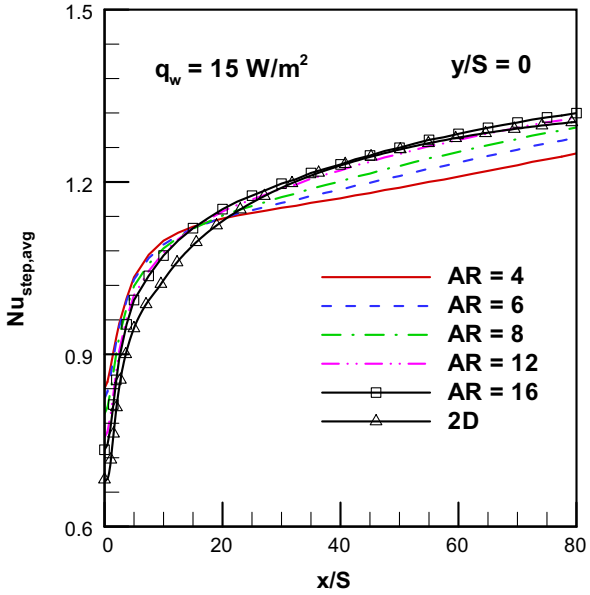

Fig. 18. Effect of aspect ratio on the streamwise distribution of the average Nusselt number.

ratio has only small effect on the average Nusselt number distribution.

4. Conclusions

The effect of buoyancy force and duct's aspect ratio on the flow and heat transfer in laminar 3-D buoyancy assisting mixed convection in plane symmetric sudden expansion is presented for the case when the flow and thermal fields are symmetric. As buoyancy level increases the size of the recirculation flow region decreases and the reattachment line moves toward the sudden expansion. A partial lifting of the reattached flow starts to develop at the center width of the duct and the lifting continues to increase with increasing level of buoyancy. Higher buoyancy level results in a higher wall and bulk fluid temperature and also a higher local and average Nusselt number. The maximum local Nusselt number develops in a region close to the side walls. Increasing buoyancy level increases the velocity and its gradient near to the stepped wall but decreases its magnitude at the center height of the duct. The temperature at the center height of the duct is not affected significantly by increasing the buoyancy level in the range of parameters that are examined in this study.

Decreasing the aspect ratio for a fixed buoyancy level causes the reattachment line to move upstream closer to the sudden expansion and initiating partial lifting of the recirculation flow region away from the stepped wall. A higher aspect ratio requires a higher buoyancy level to partially lift the recirculation flow region away from the stepped wall. The effect of the aspect ratio on the local Nusselt number near the side wall continues to be significant for ducts with large aspect ratio but that is not the case at the center width of the duct. Increasing the aspect ratio increases the local Nusselt number in the fully developed flow region near the side wall but that trend is reversed at the center width of the duct. Increasing the aspect ratio increases the maximum local Nusselt number and moves its location closer toward the side wall. The aspect ratio does not affect the bulk fluid temperature and has only a small effect on the average Nusselt number.

Acknowledgements

This work has been supported in part by a DOE-Basic Energy Sciences Grant No. DE-FG02-03ER46067, and by an NSF Grant No. CTS-0352135.

References

[1] F. Durst, A. Melling, J.H. Whitelaw, Low Reynolds number flow over a plane symmetric sudden expansion, Journal of Fluid Mechanics 64 (1974) 111–128.
[2] W. Cherdron, F. Durst, J.H. Whitelaw, Asymmetric flows and instabilities in symmetric ducts with sudden expansions, Journal of Fluid Mechanics 84 (1978) 13–31.
[3] F. Durst, J.C.F. Pereira, C. Tropea, The plane symmetric sudden-expansion flow at low Reynolds numbers, Journal of Fluid Mechanics 248 (1993) 567–581.
[4] R.M. Fearn, T. Mullin, K.A. Cliffe, Nonlinear flow phenomena in a symmetric sudden expansion, Journal of Fluid Mechanics 211 (1990) 595–608.
[5] D. Drikakis, Bifurcation phenomena in incompressible sudden expansion flows, Physics of Fluids 9 (1997) 76–87.
[6] T. Hawa, Z. Rusak, The dynamics of a laminar flow in a symmetric channel with a sudden expansion, Journal of Fluid Mechanics 436 (2001) 283–320.
[7] Y.Y. Tsui, S.J. Shu, Effects of buoyancy and orientation on the flow in a duct preceded with a double-step expansion, International Journal of Heat and Mass Transfer 41 (17) (1998) 2687–2695.
[8] S.E. Alimi, J. Orfi, S.B. Nasrallah, Buoyancy effects on mixed convection heat and mass transfer in a duct with sudden expansions, Heat and Mass Transfer 41 (2005) 559–567.
[9] M. Thiruvengadam, J.H. Nie, B.F. Armaly, Bifurcated three-dimensional forced convection in plane symmetric sudden expansion, International Journal of Heat and Mass Transfer 48 (2005) 3128–3139.
[10] M. Thiruvengadam, B. F Armaly, J.A. Drallmeier, Three-dimensional mixed convection in plane symmetric-sudden expansion: Bifurcated flow regime, ASME Journal of Heat Transfer 129 (2007) 819–826.
[11] A. Li, B.F. Armaly, Mixed convection adjacent to 3-D backward facing step, Proceedings of the ASME-IMECE Conference, ASME HTD, 366-2, New York, 2000, pp. 51–58.
[12] R. K Shah, M.S. Bhatti, Laminar convective heat transfer in ducts, in: S. Kakac, R.K. Shah, W. Aung (Eds.), Handbook of Single-Phase Convective Heat Transfer, John Wiley & Sons, New York, 1987, pp. 3.45–3.47.